

CHAPTER 5

Discussion

CHAPTER 5

DISCUSSION

The fly ash generated by the process of coal combustion in thermal power stations is being disposed off by the wet and dry methods. In both the cases the fly ash come in contact with water and heavy metals present therein are leached and contaminate the soil water environment. In the present study to assessment the leaching potential of fly ash and fly ash materials (bricks, blocks and cement) in the acidic, neutral and alkaline environment and to study the changes in metal speciation and mobility that can occur during wet storage of fly ash and fly ash materials (bricks, blocks and cement) under static conditions. In these studies, the leaching of heavy metals like Cr, Fe, Ni, Cu, Pb and Cd etc. from fly ash and its admixtures investigated to predict potential environmental pollution. The leaching of heavy metals by sequential batch leaching test (SBLT) and long term leaching test (LTLT) is a recent technique being employed in present study.

5.1 Characterization of coal

A typical X-ray diffraction spectrum of coal has been shown in Fig. 4.1 indicates that it contains both crystalline and amorphous material. The main peak at $2\theta = 26.61^\circ$ for coal corresponds to that of quartz, which indicates that quartz or silica is an important component of coal. Another mineral, kaolinite, was also found in coal samples indicated by strong peaks at $2\theta = 6.5^\circ$. This result is similar to that reported for a coal sample by Sarwar et al., 2012, Ritz and Kalika, 2010. The peak intensity of the XRD, quartz was very strong in coal samples, with kaolinite as another chemically stable component. These two constituents mask the most active internal constituents of coal comprising porous, spongy and amorphous particles. For the most part, coal particles are glassy or amorphous. The compounds of kaolinite, mikasaite, anatase, quartz, basiteite and pyrite are present in crystalline form, which is less than% by weight of carbon. The mineral identified in coal is shown in Table 4.1.

The surface topography of the coal materials was identified by scanning electron microscopic (SEM) and micrographs are shown in Fig. 4.2. SEM image of the coal reveals the amorphous nature of the coal, with particle agglomerates and distinct difference in the morphology of the samples. The coal also showed fibrous and non-porous structure with uneven topography. The coal particles are irregular in shape and exhibit conchoidal fracture lines. The surfaces appeared smooth and homogeneous.

EDS spectra showed the presence of Carbon (C), Oxygen (O), Aluminum (Al), Iron (Fe) and Silica (Si) as the major elements in the coal (Fig. 4.3). The weight % and atom % of the coal samples, as measured by EDS, are given in Table 4.2. In this case, C and O is the predominant element, but Al, Fe and Si vary widely from one type of coal to another. Generally, the elemental predominance of the coal sample is $C > O > Si > Al > Fe$. Coal is elementally composed of a high concentration of carbon and oxygen, with lighter amount of aluminum, silicon and iron.

The compositions of the coal samples obtained from XRF are given in Table 4.3. The relative distribution of the oxides in the coal samples is also shown in Fig. 4.4. The chemical composition is dominated by silica which constitutes nearly 63% by wt of the total composition. Overall, the composition of the oxides in the coal samples is in the order of $SiO_2 > Al_2O_3 > Fe_2O_3 > SO_3 > TiO_2 > K_2O > CaO > ZnO > P_2O_5 > PbO > MnO_2 > SrO > CdO$. SiO_2 , Al_2O_3 and Fe_2O_3 are the three most important constituents of the coal and they together make up 90 % by wt of the coal. The composition of the minor oxides, K_2O , CaO , TiO_2 , P_2O_5 , PbO , SrO , CdO and MnO_2 showed some variation in the coal samples, as seen. It can be seen from the Table 4.3 that the major constituents are, silica as SiO_2 about 63%, alumina as Al_2O_3 about 19% and iron oxide as Fe_2O_3 about 8%. The chemical composition of coal depends mainly on the composition of the parental rock strata and formation of coal.

The assignment of various bands for coal is given in Table 4.4. Coal samples gave IR frequencies which correspond with those reported in the literature. In assigning the bands, the absorption bands are compared with the standard patterns (Grigoriev, 1990, Karr 1978, Scheinman, 1970, Speight, 1994, Cooke et al., 1986, Das, 2001). The broad bands

around 3693 and 1032 cm^{-1} is due to – OH vibrations and is attributable to the existence of surface hydroxyl groups and chemisorbed water (Daifullah et al., 2003, Ibrahim et al., 1980). These absorptions are most useful in determining the aromatic ring structure of a coal. Most of the peaks in FT-IR spectra of coal between 1100 and 400 cm^{-1} can be assigned to clay minerals such as quartz, kaolinite, illite and the montmorillonite group. The distinct peak at 1032 cm^{-1} , 913 cm^{-1} , 797 cm^{-1} , 694 cm^{-1} , 538 cm^{-1} , 469 cm^{-1} and 432 cm^{-1} can be attributed to these mineral groups in coal sample. The Si–O–Si stretching vibration causes absorption at 1032 cm^{-1} and 1009 cm^{-1} . The Si–O bending vibration contributes to the strong absorption at 538 cm^{-1} and 469 cm^{-1} . Both these peaks can also be due to the presence of ionic sulphates. A weak absorption due to iron pyrite (FeS_2) at 432 cm^{-1} is also observed. A small but visible band at 694 cm^{-1} may possibly be due to magnetite (Fe_2O_3).

There are various types of Coals, mainly Bituminous (Marine coal, CIC field coal, Imported coal, Wash coal, Enviro coal) used in Gandhinagar Thermal Power Station for generation of electricity. There are specified parameters of various coals are given in Table 4.5. This showed that it contain total moisture (%) range from 8 to 12, inherent moisture (%) range from 4 to 6, volatile (%) range from 20 to 25 and ash (%) range from 35 to 45. GTPP consumed 37.18 MT/ Annual amount of coal and generated 12.45 MT/Annual amount of fly ash which was recorded 33.48% of total coal consumed and 9.87MT/Annual amount of fly ash is utilized.

5.2 Characterization of fly ash

Fly ash sample had X-ray diffraction patterns indicating their mineralogical compositions. The X-Ray diffractograms of the fly ash sample is given in Fig. 4.6. The major peak at $2\theta = 26.61^\circ$ for fly ash corresponds to that of quartz, indicating that quartz or silica is a major constituent of fly ash. Another mineral, mullite, illite montmorillonite was also found in the fly ash samples indicated by strong peaks. This result is similar to that reported for a fly ash sample by Jason et al., 2005. The intensity of quartz XRD peak was very strong in fly ash sample, with mullite as another chemically stable component. These two constituents mask the more active inner constituents of fly ash comprising of

porous, spongy and amorphous particles. The XRD patterns indicate that it contains both crystalline and amorphous material. About 90% of the fly ash particles are glassy or amorphous. It may be noted that several major crystalline phases, mullite ($3\text{Al}_2\text{O}_3\text{SiO}_2$), quartz (SiO_2) and illite montmorillonite ($\text{KA1}_4(\text{Si}, \text{Al})_8\text{O}_{10}$) have been identified in fly ash sample through XRD analysis (Hackel et al., 2008; Kastner et al., 2008) which constitutes about 10-15% by weight of fly ash. The mineral identified in fly ash is shown in Table 4.6.

The SEM micrographs of the fly ash sample are shown in Fig. 4.7 (a, b and c). The particle size observed in this study ranged from less than $1\mu\text{m}$ to more than $200\mu\text{m}$. Most of the particles varied in size from about 1 to $100\mu\text{m}$ and consisted of solid spheres (Fig. 4.7a). The hollow cenosphere (Fig. 4.7b) and the unburned carbon particles of irregular shape (Fig. 4.7c) tended to be at the upper end of the size distribution. The SEM image of the fly ash reveals the amorphous nature of the ash, with agglomerations of particles and a clear difference in the morphology of the sample. The figure indicates that the main particle is hollow (sponge sharp) but attached with other particles. The fly ash also showed a fibrous and porous structure with irregular topography. The figure clearly illustrates that the particles in the windward direction are larger and hollow in the structure, while the particles in the direction of the lean are almost spherical in nature, smaller in size and more homogeneous with respect to the particles in the windward direction.

EDS spectra showed the presence of Oxygen (O), Aluminum (Al) and Silica (Si) as the major elements in the fly ash (Fig. 4.8). The weight % and atom % of the coal samples, as measured by EDS, are given in Table 4.7. In this case O is the predominant element, but Al, Fe and Si vary widely from one type of fly ash to another. Generally, the elemental predominance of the fly ash sample is $\text{O} > \text{C} > \text{Al} > \text{Si} > \text{Fe}$. Fly ash is elementally composed of a high concentration of oxygen, with lighter amount of aluminum, silicon, iron, potassium, sodium, magnesium and titanium. Wu and Ting, 2006 reported that the most abundant elements present in fly ash were O, Al, Si, C, K and calcium. The high concentration of these elements was due to the formation of metal oxides and to the treatment with lime spray during the incineration process. Most of these main

constituents become part of the fly ash during high-temperature coal combustion. On the other hand, most of the minor constituents of fly ash are heavy metals which include Fe, Pb, Cd, Co, Cr, Ni, Ba, Ti and Zn which are found in small amounts in the fly ash (Kida et al., 1996).

The chemical compositions of the fly ash samples obtained from XRF are given in Table 4.8. The relative distribution of the oxides in the fly ash samples is also shown in Fig. 4.9. Fly ash mainly consists of Silica (SiO_2), Alumina (Al_2O_3), Calcium Oxide (CaO), and Iron Oxide (Fe_2O_3). The fly ash has a high loss on ignition (LOI) value, indicating that the sample still contained some amount of volatile materials (must be organic in nature). The chemical composition is dominated by silica which constitutes nearly 60% by wt of the total composition. Overall, the composition of the oxides in the fly ash samples is in the order of $\text{SiO}_2 > \text{Al}_2\text{O}_3 > \text{Fe}_2\text{O}_3 > \text{Na}_2\text{O} > \text{TiO}_2 > \text{K}_2\text{O} > \text{CaO} > \text{MnO} > \text{Cr}_2\text{O}_3 > \text{SO}_3 \sim \text{V}_2\text{O}_5 > \text{CuO} > \text{ZnO} > \text{SrO} > \text{CoO} > \text{As}_2\text{O}_5 > \text{NiO} > \text{Br}_2\text{O}$. SiO_2 , Al_2O_3 and Fe_2O_3 are the three most important constituents of fly ash and they together make up 89 % by wt of the fly ash. The composition of the minor oxides, Na_2O , K_2O , CaO , MnO , Cr_2O_3 , TiO_2 , SrO , CoO , NiO , As_2O_5 and Br_2O show some variation in the fly ash samples, as seen. The composition of fly ash is shown in Table 4.8. From the table it can be observed that the main constituents are silica such as SiO_2 about 60%, alumina as Al_2O_3 about 25% and iron oxide like Fe_2O_3 about 5%. The chemical composition of fly ash depends mainly on the composition of parent coal and coal combustion conditions.

The assignment of various bands for fly ash is given in Table 4.9. Fly ash samples gave IR frequencies which correspond with those reported in the literature. In assigning the bands, the absorption bands are compared with the standard patterns (Summer, M.E., 1995, Ktara et al., 2013, Ramasamy et al., 2006 and Russell, J. D., 1987). Bands were observed in the IR spectra of fly ash sample at around 3484, 1094, 795, 558 and 463 cm^{-1} . A broad absorption band is observed at 1094 cm^{-1} in the fly ash, which appears to be mainly due to Si-O-Si asymmetric stretching vibration. The FTIR spectrum of quartz has peaks at 1094 and 795 cm^{-1} (Ktara et al., 2013). It is clear that many of the peaks in the spectrum of fly ash overlap with that of glass and quartz. The strongest peak in the fly ash

spectrum observed around 1094 cm^{-1} is attributed Si-O-Si asymmetric stretching vibrations and has contributions of glass, mullite and quartz. The band at 795 cm^{-1} is attributed to Si-O symmetric stretching vibrations from quartz (Ktara et al., 2013). Si-O-Al symmetrical stretching vibrations occur at about 558 cm^{-1} (Ramasamy et al., 2006) and overlaps of the very characteristic of hematite at 558 cm^{-1} . The 463 cm^{-1} peak belongs to amorphous silica Si-O-Si band (feldspar) and the 3484 cm^{-1} peak to OH group of adsorbed water dust-stretching.

The wide range of particle size distribution in fly ash is shown in Fig.4.11. The results showed that fly ash contains more fine particles sized small than 4580 nm . The particle size distribution curve shows the presence of particles of size ranging from 3150 nm and 4580 nm . Fly ash has approximately 50% of particle sized lower than 3670 nm . Particle size distribution is the physical characteristics of the fly ash which is mostly affect their reactivity and their use as pozzolans. Pozzolanic reaction property increases with the increase of fineness properties (Demir et al., 2002). The fineness of fly ash is affected by pulverisation of coal, thermal process and type of electrostatic precipitator installed in power station.

The physico-chemical analysis of fly ash samples (Table 4.11) shows that the fly ashes of GTPP contain moisture between 8 and 10 %, organic carbon range from 0.32 to 1.47 and EC ($\mu\text{s/m}$) between 441 and 467. The fly ash shows pH values between 7.82 and 8.02. Water holding capacity of fly ash was 42 to 46%, porosity was 50 to 54%. Specific gravity of fly ash was 1.23 to 1.27 and loss of ignition (LOI) was 1.8-2.2%. The bulk density of fly ash was recorded $1.26\text{ to }1.32\text{ g/cm}^3$. The colour of fly ash was light grey and particle shape was spherical with irregular. Grain size of fly ash was major fine sand/silt and small percent of clay.

5.3 Heavy metals in coal and fly ash

The results for the heavy metal analysis of coal and fly ash samples are given in Table 4.10. Results of the selected heavy metals showed that Cr, Fe, Ni, Cu, Zn, As, Cd and Pb are present on the particle surfaces, though their concentration vary widely among both samples (Fig.4.12). The concentrations ($\mu\text{g/g}$) of toxic elements Cr, Fe, Ni, Cu, Zn, As,

Cd and Pb found 57.14, 830.62, 32.34, 52.21, 75.78, 2.10, 1.92 and 23.46 in coal, 80.20, 902.55, 39.49, 68.54, 94.00, 5.54, 3.10 and 30.68 in fly ash respectively. Among the trace elements, it was found that the elements are present in coal and fly ash samples in the order of $Fe > Zn > Cr > Cu > Ni > Pb > As > Cd$. The elements are more concentrated in case of fly ash than coals. This variation may be ascribed to the fineness of fly ash particles with large surface ratio to mass preferentially concentrate more these elements.

5.4 Characterization of dry and wet disposal fly ash

Both disposal fly ash samples had similar X-ray diffraction patterns indicating similarity in their mineralogical compositions. The X-Ray diffractograms of the both disposal fly ash samples are given in Fig.4.13 (a) and (b). The major peak at $2\theta = 26.94^\circ$ ($d = 3.30 \text{ \AA}$) for both dry disposal fly ash and wet disposal fly ash, corresponds to that of quartz, indicating that quartz or silica is a major constituent of disposal fly ash. Another mineral, illite-montmorillonite was also found in the dry disposal fly ash samples. The intensity of quartz XRD peak was very strong in each of the disposal fly ash samples, with illite as another chemically stable component. These two constituents mask the more active inner constituents of fly ash comprising of porous, spongy and amorphous particles. The XRD patterns also reveal that fly ash is a largely amorphous glassy material.

The surface topography of the disposal fly ash materials was identified by SEM and micrographs are shown in Fig.4.14 (a and b) respectively for dry and wet disposal fly ash. SEM image of the fly ash reveals the amorphous nature of the ash, with particle agglomerates and distinct difference in the morphology of the samples. The fly ash also showed fibrous and porous structure with uneven topography. The microstructure of dry disposal fly ash shows the typically well rounded, solid spheres, and the larger particles size. The wet disposal fly ash image shows the agglomeration texture of wet disposal fly ash. Wet disposal fly ash exposes a compact structure of the fly ash particles, variety of pores with a heterogeneous distribution of pore diameters.

EDS spectra of disposal fly ash sample show strong peaks due to oxygen, silicon, aluminium and carbon and very weak peaks due to iron, magnesium, potassium and calcium (Fig.4.15 a, b). EDS spectra showed the presence of O, Al, and Si as the major

elements in the disposal fly ash (Fig.4.15 a, b). The weight % and atom % of the disposal fly ash samples, as measured by EDS, are given in Table 4.13. In both cases, O is the predominant element, but Si and Al vary widely from one type of fly ash to another. Generally, the elemental predominance of the fly ash samples is $O > Si > Al$.

The compositions of the dry and wet disposal fly ash obtained from XRF are given in Table 4.14. The relative distribution of the oxides in the disposal fly ash samples is also shown in Fig.4.16 a, b. XRF spectra show the presence of Si, Al, Fe, Na, Ti, K, Ca, Mn, S, V, Cu, Zn, Sr, Co, As, Ni and Br as the bulk oxide of major elements in the dry and wet disposal fly ash samples. The dry disposal fly ash has a very high loss on ignition (LOI) value, indicating that the sample still contained some amount of volatile materials (must be organic in nature). This must have accumulated during the time when the fly ash was kept dumped on soil. Very little LOI in wet disposal fly ash samples indicates that the disposal operation (by water) removed most of the volatile material from the fly ash. The chemical composition is dominated by silica which constitutes nearly 72 to 76% by wt of the total composition. Overall, the composition of the oxides in the fly ash samples is in the order of in **DDFA**: $SiO_2 > Al_2O_3 > Fe_2O_3 > TiO_2 > K_2O > CaO > MnO_2 > SO_3 > CuO > SrO > ZnO > V_2O_5 > CoO > As_2O_5 > NiO > Br_2O > Cr_2O_3$ and in **W DFA**: $SiO_2 > Al_2O_3 > Fe_2O_3 > TiO_2 > K_2O > CaO > Cr_2O_3 > MnO_2 > V_2O_5 > ZnO > CoO > SrO > Br_2O > As_2O_5 > NiO$. SiO_2 , Al_2O_3 and Fe_2O_3 are the three most important constituents of dry and wet disposal fly ash and they together make up 93 to 96 % by wt of the disposal fly ash. The composition of the minor oxides, TiO_2 , K_2O , CaO , Cr_2O_3 , MnO_2 , V_2O_5 , ZnO , CoO , SrO , Br_2O , As_2O_5 , and NiO show some variation among the disposal fly ash samples, as seen. The composition of dry and wet disposal fly ash is shown in Table 4.14. It can be seen from the table that the major constituents are, silica as SiO_2 , alumina as Al_2O_3 and iron oxide as Fe_2O_3 . Oxides of calcium, magnesium, potassium, chromium, sulfur, titanium, vanadium and arsenic are also present in small amounts.

The assignment of various bands for dry and wet disposal fly ash is given in Table 4.15 and 4.16. Fly ash samples gave IR frequencies which correspond with those reported in the literature. The IR bands for DDFA appear at 1091 cm^{-1} (denoting to Si-O-Si asymmetric stretching vibration), 794 cm^{-1} (Si-O symmetric) and band at 550 cm^{-1} (Si-O–

Al). The IR bands for W DFA appear at 3459 cm^{-1} (denoting to H-O-H stretching of water molecules), $2858, 2922\text{ cm}^{-1}$ (C-H stretching vibration), 1640 cm^{-1} (C=O carboxylate group of organic matter), 1081 cm^{-1} (Si-O stretching of clay mineral) and band at 781 cm^{-1} (C-H bending) (Summer, M.E., 1995, Ktara et al., 2013, Ramasamy et al., 2006 and Russell, J. D., 1987).

The colour of dry fly ash was grey where colour of wet fly ash was dark grey and particle shape was spherical with irregular. Grain size of dry and wet fly ash was fine sand /silt and major fine sand/silt with small percent of clay respectively. Both dry and wet disposal fly ash show alkaline nature.

5.5 Heavy metal in dry and wet disposal fly ash

Dry and wet disposal fly ash samples were analyzed for chromium (Cr), iron (Fe), nickel (Ni), copper (Cu), zinc (Zn), arsenic (As), cadmium (Cd). The results for the heavy metal analysis of dry and wet disposal fly ash are given in Table. 4.17. Results of the selected heavy metals showed that Cr, Fe, Ni, Cu, Zn, As, Cd and Pb are present on the particle surfaces, though their concentration vary widely among both samples (Fig.4.18). The concentrations ($\mu\text{g/g}$) of toxic elements Cr, Fe, Ni, Cu, Zn, As, Cd and Pb found 68.43, 710.52, 33.73, 59.62, 83.54, 3.36, 2.52 and 24.37 in dry disposal fly ash, 58.34, 612.25, 19.63, 57.14, 70.80, 2.43, 2.10 and 20.55 in wet disposal fly ash respectively. Among the trace elements, it was found that the elements are present in dry and wet disposal fly ash samples in the order of $\text{Fe} > \text{Zn} > \text{Cr} > \text{Cu} > \text{Ni} > \text{Pb} > \text{As} > \text{Cd}$. The elements are more concentrated in case of dry disposal fly ash than wet disposal fly ash. A comparison of the results with the values, for fly ash, dry and wet disposal fly ash are shown in Table 4.18 and Fig.4.19. This comparison result show that present of elements in order of Fly ash (FA) > Dry disposal fly ash (Ash dyke) > Wet disposal fly ash (Pond ash)

5.6 Physico-chemical characteristics of fly ash effluent at fly ash disposal pond

The seasonal variations in physico-chemical characteristics of the fly ash effluent water sample have been summarized in the Table 4.20, 4.21 and 4.22. Analytical results revealed physicochemical characteristics of fly ash effluent water samples from five

locations of the ash pond during winter, summer and monsoon season. The physico-chemical properties of the ash effluents like temperature, pH, TDS, electrical conductivity, alkalinity, total hardness, calcium hardness, magnesium hardness, chloride, sulphate, phosphate, ammonia-nitrogen, nitrite-nitrogen and nitrate-nitrogen showed significant varied from the discharge point towards the stagnant water collected from the western boundary. pH, alkalinity, total hardness and phosphate recorded a slight increase at the stagnant water area, TDS of ash effluent showed sharp decline after 300m distance from disposal point due to settling of fly ash particles, Cl⁻ concentration decreased after 300m of effluent flow. Concentration of ammonia-nitrogen, nitrite-nitrogen and nitrate-nitrogen from different sampling sites in the disposal pond varied significantly. All these parameters varied with season and variations were across the sampling site.

5.6.1 Temperature

The average effluent water temperature varied from $22.62 \pm 0.47^{\circ}\text{C}$ to $33.30 \pm 0.69^{\circ}\text{C}$. Effluent water temperature ranged between 22.10 - 22.80, 32.60 - 34.30 and 30.40 - 30.90°C, with mean value of 22.62 ± 0.47 , 33.30 ± 0.69 and $30.70 \pm 0.19^{\circ}\text{C}$ during winter, summer and monsoon season respectively in the ash pond. Effluent water temperature was found lower in the winter than that of monsoon and summer season in the ash pond (Fig. 4.20). This investigation is also similar conformity with the finding of Moundiotiya et al., 2004, Mishra et al., 2008, Sharma and Capoor, 2010 and Arya et al., 2011.

5.6.2 pH

In all effluent water samples, the pH values ranged from 7.99 – 8.17, 7.39 – 8.04 and 7.73 – 8.85 and with mean value of 8.02 ± 0.12 , 7.63 ± 0.29 and 7.96 ± 0.21 during winter, summer and monsoon season respectively in the ash pond. pH varied with seasons and variations were across the sampling site. The pH of water was relatively high in the winter months and low in the summers and monsoon. The similar results were reported by Salam et al., 2000, Mishra et al., 2008, Sharma and Capoor, 2010 and Arya et al., 2011. The results indicate that the fly ash effluent water samples are alkaline in nature. This is due to the nature of feed coal itself (alkaline fly ash). This is in striking contrast

with the much higher (>7.9) reported mean values of ash pond effluents at Farraka and Bhandal (West Bengal) as well as Bhusawal and Chandrapur (Maharashtra), Rudra et al., 1998.

5.6.3 Electrical conductivity

The EC ranged from 708 – 776, 787 – 846 and 715 – 832 $\mu\text{s}/\text{m}$ and with mean value of 729.6 ± 26.76 , 806.6 ± 25.27 and 775.4 ± 25.11 $\mu\text{s}/\text{m}$ during winter, summer and monsoon season respectively in the ash pond. The conductivity values were observed to be less at ash pond in winter than the summer and monsoon season. No significant variation was recorded at either of the outlets during period of sampling. The vast difference in conductivity values between sites may perhaps be due to reduced retention times and lack of efficiency of filters used in decantation towers in the latter areas. The fluctuations in electric conductivity are due to fluctuation in total dissolved solids and salinity (Boyd, 1981).

5.6.4 Total dissolved solids

The TDS ranged from 354 – 386, 394 – 409 and 357 – 417 mg/l and with mean value of 364.6 ± 12.42 , 403.4 ± 12.24 and 387.6 ± 25.11 mg/l during winter, summer and monsoon season respectively in the ash pond. The value of total dissolved solid was higher during the summer season and it decreases during winter season (Fig.4.20). This observation also supports the findings of Moundiotiya et al., 2004, Salam et al., 2000 and Mishra et al., 2008. Total dissolved solids in the most of the cases are organic in nature and pose serious problems of pollution (Trivedi et al., 1987).

5.6.5 Total alkalinity

Total alkalinity ranged from 168 – 212, 244 – 320 and 176 – 182 mg/l and with mean value of 198.2 ± 17.70 , 281.6 ± 27.03 and 179.6 ± 2.33 mg/l during winter, summer and monsoon season respectively in the ash pond. Alkalinity was high during the summer season followed by monsoon and winter season. The result also supports the findings of Mishra et al., 2008 and Arya et al., 2011.

5.6.6 Total Hardness

Total hardness concentration with mean value of 236 ± 8.37 , 243.6 ± 7.13 and 227.2 ± 7.86 mg/l as CaCO_3 during winter, summer and monsoon season respectively in the ash pond. The Ca hardness ranged with mean value of 151.2 ± 5.93 , 154.6 ± 4.34 and 144.6 ± 7.14 mg/l as CaCO_3 during winter, summer and monsoon season respectively in the ash pond. The Mg hardness ranged with mean value of 84.80 ± 3.63 , 87.00 ± 3.32 and 82.6 ± 5.64 mg/l as CaCO_3 during winter, summer and monsoon season respectively in the ash pond. The season of summer exhibited maximum total hardness and the season of monsoon exhibited minimum total hardness (Fig.4.20). Khan et al., 1986 studied the total hardness in different reservoirs during the different season and showed that the total hardness varied from reservoir to reservoir due to their geological setting.

5.6.7 Chloride

The chloride ranged from 83 – 88, 92 – 102 and 86 – 98 mg/l and with mean value of 85.00 ± 2.00 , 96.60 ± 3.71 and 92.00 ± 4.56 mg/l during winter, summer and monsoon season respectively in the ash pond. The chloride content was at its maximum in summer and lowers down during winter season (Fig.4.20). The higher concentration of Chloride is considered to be an indicator of higher pollution due to higher organic waste of animal origin. The result also supports the findings of Moundiotiya et al., 2004, Mishra et al., 2008 and Arya et al., 2011. The concentration of higher chloride in the summer season could be also due to increased temperature and evaporation by water.

5.6.8 Sulphate

The sulphate ranged from 34 – 40, 42 – 50 and 52 – 60 mg/l and with mean value of 36.40 ± 2.61 , 46.80 ± 3.03 and 56.00 ± 2.83 mg/l during winter, summer and monsoon season respectively in the ash pond. From the Table 4.23 it is obvious that the sulphate concentrations are more or less similar to chloride values during the years of sampling. Sulphate level of 21 mg/l at ash pond, Bhandal (West Bengal) and 25 mg/l at ash pond, Chandrapur (Mharasrta) were reported by Rudra et al., 1998.

5.6.9 Phosphate

The phosphate ranged from 1.20 – 1.80, 1.80 – 3.80 and 1.60 – 2.40 mg/l and with mean value of 1.44 ± 0.26 , 2.84 ± 0.82 and 2.04 ± 0.29 mg/l during winter, summer and monsoon season respectively in the ash pond. Phosphate concentrations were found to be less in winter and maximum in summer season (Fig.4.20). Marginally higher levels at points of discharge are attributed to the contribution from of fly ash. Much higher value 2.4 to 3.8 mg/l observed at ash pond is probably a result of anthropogenic input in the form of fertilizers used for cultivation on the banks of Sabarmati River. These are, however, much lesser than the values observed at ash pond Bhandal, Bhusawal, Chandrapur and Farraka where mean values are in the range of 9.5 to 12.3 mg/l (Rudra et al., 1998)

5.6.10 Ammonia-nitrogen

The ammonia-nitrogen ranged from 0.78 – 0.86, 0.52 – 0.64 and 0.40 – 0.52 mg/l and with mean value of 0.83 ± 0.03 , 0.58 ± 0.04 and 0.46 ± 0.05 mg/l during winter, summer and monsoon season respectively in the ash pond. The appearance of ammonia in the waters can be accepted as the chemical test of organic contamination (Trivedi and Goel, 1984). Naturally in unpolluted ponds, the concentration of NH_4^+ is generally higher during winter season because the nitrification process in the pond is more affected at higher temperature in summer season (Haag and Westrich, 2002).

5.6.11 Nitrite-nitrogen

The nitrite-nitrogen ranged from 0.042 – 0.048, 0.034 – 0.040, and 0.030 – 0.038 mg/l and with mean value of 0.05 ± 0.00 , 0.04 ± 0.00 and 0.03 ± 0.00 mg/l during winter, summer and monsoon season respectively in the ash pond. Nitrite-nitrogen always indicates the fresh entry of organic load in to the water system (Sundaray et al., 2005). The concentration of nitrite-nitrogen was higher in winter season, which is due to the inflow of municipal sewage from township. The nitrite-nitrogen discharge through effluents during indicates that the concentration is diluted during winter season.

5.6.12 Nitrate-nitrogen

The nitrate-nitrogen ranged from 0.95 – 1.18, 1.18 – 1.42, and 0.86 – 0.92 mg/l and with mean value of 1.11 ± 0.10 , 1.34 ± 0.10 and 0.89 ± 0.02 mg/l during winter, summer and monsoon season respectively in the ash pond. In the present study maximum nitrate-nitrogen content was found in summer season i.e. 1.34 ± 0.10 mg/L and minimum nitrate-nitrogen content was found in monsoon season i.e. 0.89 ± 0.02 mg/L (Table 4.23). The concentration of nitrate-nitrogen concentration increases due to influx of nitrogen rich flood water that brings about large amount of contaminated sewage water and also increases the concentration of nitrate- due to the formation of blooms (Verma, 2012). The concentration of nitrate-nitrogen is found higher in because of runoff of nitrate rich fertilizers and animal manure into the ash pond.

5.7 Assessment of heavy metal contents in fly ash effluent at fly ash disposal pond

The seasonal variations in heavy metal contents of the fly ash effluent water sample have been summarized in the Table 4.24, 4.25 and 4.26. Analytical results revealed heavy metal contents in fly ash effluent water samples from five locations of the ash pond during winter, summer and monsoon season. The heavy metal contents of the ash effluents like arsenic (As), cadmium (Cd), chromium (Cr), copper (Cu), iron (Fe), nickel (Ni), lead (Pb) and zinc (Zn) showed significant varied from the discharge point towards the stagnant water collected from the western boundary. All these heavy metals concentration varied with season and variations were across the sampling site.

5.7.1 Arsenic

The mean concentration of arsenic were 1.56 ± 0.15 , 4.2 ± 0.05 and 3.65 ± 0.28 $\mu\text{g/L}$ during winter, summer and monsoon season respectively in the ash pond. Arsenic concentrations were found to be less in winter and maximum in summer followed by monsoon season. Ash pond concentrations were, however, observed to be well within the permissible limit of $50\mu\text{g/L}$ (IS 2296-class A, 1982), and very much less than $10\mu\text{g/L}$ mean value estimated by Rudra et al., 1998 at ash pond, Farraka.

5.7.2 Cadmium

The mean concentrations of cadmium were 1.19 ± 0.02 , 1.63 ± 0.02 and $1.34 \pm 0.04 \mu\text{g/L}$ during winter, summer and monsoon season respectively in the ash pond. Cadmium concentrations were found to be less in winter and maximum in monsoon followed by summer season. Ash pond concentrations were, however, observed to be well within the permissible limit of $10 \mu\text{g/L}$ (IS 2296-class A, 1982). According to Rudra et al., 1998 the mean cadmium concentration was less than the permissible limit at all places analysed except for Chadrapur where it was as high as $25 \mu\text{g/L}$.

5.7.3 Chromium

Seasonal variations were observed in chromium concentrations, in ash pond. The mean concentrations of cadmium were 3.76 ± 0.16 , 7.31 ± 1.05 and $4.05 \pm 0.13 \mu\text{g/L}$ during winter, summer and monsoon season respectively in the ash pond. Cadmium concentrations were found to be maximum in summer and minimum in winter season. Ash pond concentrations were, however, observed to be well within the permissible limit of $50 \mu\text{g/L}$ (IS 2296-class A, 1982). The result is also in close conformity with the findings of Rudra et al., 1998). Chromium concentrations in ash pond effluents were below the detection limit at Farraka, Bhandar, Bhusawal and Chandrapur (Rudra et al., 1998).

5.7.4 Copper

Copper concentrations were observed with mean value of 55.62 ± 0.85 , 71.59 ± 1.27 and $60.59 \pm 0.38 \mu\text{g/L}$ during winter, summer and monsoon season respectively in the ash pond. During summer season, it was found in the range of $70.66 - 73.33 \mu\text{g/L}$ which is higher than monsoon and winter season. The reason may be attributed to the leaching in the feed coal and in fly ash during summer. However, it was observed that ash pond concentrations were within the permissible limit of $1500 \mu\text{g/L}$ (IS 2296 class A, 1982), and is higher than the values estimated by Rudra et al., 1998 at ash pond Farraka, Bhandal (Waste of Bengal), Bhusawal and Chandrapur (Maharashtra).

5.7.5 Iron

The Fe ranged from 112.84 – 122.52, 156.32 – 200.14, and 132.28 – 166.62 $\mu\text{g/L}$ and with mean value of 117.17 ± 3.57 , 176.01 ± 25.82 and 148.12 ± 12.25 $\mu\text{g/L}$ during winter, summer and monsoon season respectively in the ash pond. The maximum Fe concentration 207.35 $\mu\text{g/L}$ was observed in summer and minimum value 112.84 $\mu\text{g/L}$ in the winter season. However, it was observed that ash pond concentrations were within the permissible limit of 300 $\mu\text{g/L}$ (IS 2296 class A, 1982).

5.7.6 Nickel

Nickel concentration ranged from 4.80 – 15.64, 18.30 – 32.04, and 16.13 – 22.56 $\mu\text{g/L}$ and with mean value of 9.82 ± 4.33 , 24.35 ± 5.37 and 18.73 ± 2.47 $\mu\text{g/L}$ during winter, summer and monsoon season respectively in the ash pond. The maximum nickel concentration was observed in summer and minimum in the winter season.

5.7.7 Lead

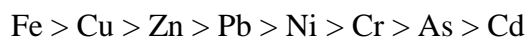
The Pb concentration ranged from 4.80 – 15.64, 18.30 – 32.04, and 16.13 – 22.56 $\mu\text{g/L}$ and with mean value of 9.82 ± 4.33 , 24.35 ± 5.37 and 18.73 ± 2.47 $\mu\text{g/L}$ during winter, summer and monsoon season respectively in the ash pond. During winter season, it was found in the range of 4.80 – 15.64 $\mu\text{g/L}$ which is less than the summer season concentrations in range of 18.30 – 32.04 $\mu\text{g/L}$. However, it was observed that ash pond concentrations were within the permissible limit of 100 $\mu\text{g/L}$ (IS 2296 class A, 1982). The value recorded in the study area is much higher than the concentration observed by Rudra et al., 1998 in ash pond at Farraka, Bhandal (Waste Bengal), effluent in ash (3 and 10 $\mu\text{g/L}$) and in Bhusawal and Chandrapur (Maharashtra) (8 and 5 $\mu\text{g/L}$). The reason could be a high dilution of fresh water used for the slurry and variation of the feed coal.

5.7.8 Zinc

Concentrations of Zinc were found in the ranged from 48.33 – 55.54, 63.71 – 75.26, and 52.74– 65.43 $\mu\text{g/L}$ and with mean value of 52.01 ± 3.35 , 68.32 ± 4.38 and 59.31 ± 5.21 $\mu\text{g/L}$ during winter, summer and monsoon season respectively in the ash pond. As can be seen, the maximum Zn concentration was observed in summer and minimum in winter

season. Zinc concentrations at ash pond were observed within the permissible limit of 1500 µg/L (IS 2296-class-A, 1982). The result also supports the findings of Rudra,et al., 1988. Rudra,et al., 1988 reported that the mean vale of ash pond effluents was 150µg/L at Farakka which nearer to the observed value of the study area.

It was observed that all the trace element concentrations were found higher in summer season. Iron, copper and zinc found higher in summer season where as it were recorded low in winter seasons. Probably the change in riverine activity (wash off, precipitation, change in pH) could be the reason for reduced concentration. The reason may be increase in solubility of trace elements due to variation of pH in surface water samples and variation of supply in feed coal. The trends of trace elements during the winter, summer and monsoon seasons was as follows



5.8 Characterization of fly ash materials (bricks, blocks and cement)

In present study the leaching test were conducted on fly ash materials such as fly ash bricks, fly ash blocks and fly ash cements. Before the leaching test these fly ash materials were characterized by different advance instrumentation and their characterization briefly discussed.

X-ray diffraction analysis was performed to obtain crystalline nature and mineral composition present in the fly ash materials. XRD patterns of fly ash bricks, blocks and cements illustrated in Fig.4.23, 4.28 and 4.33 respectively. XRD patterns of fly ash bricks show that the bricks materials are prevailingly of X-ray amorphous character where the diffraction crystals were those of the original materials mainly berlinite. An amorphous hump is observed in the diffraction pattern between 2θ values of approximately 20° to 30°, which could be due to the presence of amorphous glassy materials. XRD patterns of the AAC blocks show that the AAC samples yield maximum peaks in the range of 1-60° (2θ). The major peak for AAC corresponds to that quartz that is a major constituent of AAC. Another mineral tobermorite was also found in the AAC sample indicated by strong peaks. XRD patterns of the FAC show that major peak for FAC corresponds to

that of di and tricalcium silicate that is a major constituent of FAC. Another mineral, tricalcium aluminate, tetracalcium aluminoferrite was also found in the FAC sample indicated by strong peaks.

The surface topography of the fly ash materials was identified by scanning electron microscopic (SEM). The SEM micrographs of FAB, AAC and FAC are shown in Fig. 4.24, 4.29 and 4.34 respectively. SEM image of the FAB reveals the particles are spherical in shape and were homogeneous. The micro structure of fly ash brick powder also shows the complex formation of molecules indicating no porous formation. The brick-powder particles were fused well together and cavities were present in them. Whereas SEM image of the AAC sample reveals the crystalline nature of the sample with a compact structure of the particles. ACC sample exhibited smoother surface with much smaller porosity as shown in Fig.4.29. There are no cracks observed on the surface of denser AAC samples. SEM image of the FAC reveals the amorphous natures of sample with particles are circular and spherical in shape. Shapes of cement particle were found to be also angular with non-uniformed shapes. The surfaces were rough with sharp corners.

The elemental composition of the fly ash materials was studied by EDS. EDS spectra showed the presence of O, Si, Al, and Ca as the major elements in the fly ash materials (Fig.4.25, 4.30 and 4.35). The weight % and atom % of the fly ash materials, as measured by EDS, are given in Table (4.29, 4.33 and 4.37). Fly ash bricks are elementally composed of a high concentration of oxygen, aluminum, carbon and silicon with lighter amount of iron, sodium, magnesium, titanium, potassium and calcium (Fig. 4.29). The elemental predominance of the FAB materials is $O > Al > C > Si > Na > Ti > Mg > Ca > Fe > K > Cl$. In this case, O is the predominant element, but C, Si and Al vary widely from one type of FAB materials. EDS spectra of AAC showed strong peaks due to oxygen, calcium, silicon and aluminium and very weak peaks due to iron (Fig.4.33). In this case, O is the predominant element, but Al, Fe, Ca, C and Si vary widely in AAC sample. Overall, the elemental composition of AAC materials in the order of $O > C > Ca > Si > Al > Fe$. EDS spectra of FAC (Fig. 4.37) showed the minerals present in the fly ash cement sample are oxygen, carbon, calcium, silica, aluminium, iron and magnesium. In this case, C and O is the predominant element, but Ca, Al, Fe and Si vary widely in

sample. Generally, the elemental predominance of the FAC sample is $O > C > Ca > Si > Al > Fe$. FAC is elementally composed of a high concentration of carbon and oxygen, with lighter amount of calcium, aluminum, silicon and iron.

The compositions of the fly ash materials obtained from XRF are given in Table 4.30, 4.34 and 4.38. The relative distribution of the oxides in the fly ash materials is also shown in Fig.4.26, 4.31 and 4.36. XRF spectra show the presence of Si, Al, Fe, Ti, K, Ca, Mn, Zn, Sr, Cr, Mg, Ni, Cu, As and Pb as the bulk oxide of major elements in the fly ash materials. The chemical composition of fly ash bricks and blocks is dominated by silica which constitutes nearly 50% by wt of the total composition, whereas the calcium oxide (CaO) is dominated in fly ash cements which constitute nearly 40% by wt of the total composition. Overall, the composition of the oxides in the fly ash materials in the order of

FAB: $SiO_2 > Al_2O_3 > CaO > Fe_2O_3 > TiO_2 > SO_3 > MgO > Na_2O > K_2O > MnO_2 > Cr_2O_3 > ZnO$

AAC: $SiO_2 > CaO > Al_2O_3 > SO_3 > Fe_2O_3 > TiO_2 > MgO > K_2O > ZnO > MnO_2 > PbO > SrO >$

FAC: $CaO > SiO_2 > Al_2O_3 > Na_2O > Fe_2O_3 > MgO > SO_3 > TiO_2 > K_2O > P_2O_5 > SrO > Cr_2O_3$

SiO_2 , Al_2O_3 , CaO and Fe_2O_3 are the four most important constituents of fly ash materials and they together make up 80 to 90 % by wt of the fly ash materials. The chemical composition of FA Bricks and Blocks depends mainly on the composition of fly ash, gypsum and calcium oxide and the chemical composition of FA Cement depends mainly on the composition of fly ash, lime and raw materials.

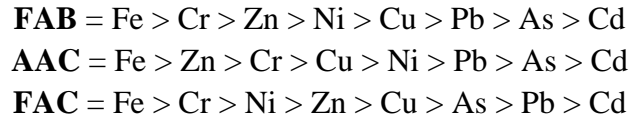
FTIR investigation has been carried out to obtain information regarding functional groups of fly ash materials. The result of FTIR of fly ash materials shown in Fig. 4.27, 4.32 and 4.37 while Table 4.31, 4.35 and 4.39 lists the position of wave numbers for molecular vibrations of different bonds that are present in fly ash materials with their possible assignments. Assignment of bands to different structural features is done as per Farmer, 1979. The IR spectrum of FAB shows the significant broad bands were observed at the

3420, 1484 and 1084 cm^{-1} for stretching vibrations of O-H, asymmetric stretching vibration of Si-O and asymmetric stretching vibration of Al-O respectively. Peaks at the 874, 855 and 795 cm^{-1} respectively, attributed to the Si-OH stretching, Al-O-H bending and stretching vibration quartz of Si-O-Si (Lyon, 1967). Additionally, the peak at 692 cm^{-1} was associated with the presence of Si-O vibration. The FTIR spectra of fly ash blocks showed a band of great intensity at 1638 cm^{-1} with a shoulder at 3465 cm^{-1} and 1446 cm^{-1} together with the bands that appeared at 1087, 971, 874, 798, 778 and 694 cm^{-1} wave numbers. The band at 3465 cm^{-1} is addressed to stretching vibrations of OH. The mid-IR bands for AAC appear at 1638 cm^{-1} (denoting to H-O-H bending of adsorbed water), 1446 cm^{-1} (aromatic -C=C stretching vibrations), 1087 cm^{-1} (Al-Si-O of amorphous aluminosilicates). The FTIR spectra of fly ash cements showed a band of great intensity at 1427 cm^{-1} with a shoulder at 3642 cm^{-1} together with the bands that appeared at 995, 923, 876, 659, 519 and 459 cm^{-1} wave numbers were associated with formation of sodium-calcium-carbonate. The band at 3642 cm^{-1} is addressed to stretching vibrations of Ca-OH from portlandite. The mid-IR bands for FAC appear at 1427 cm^{-1} (denoting to asymmetric stretching of CO_3^{2-}), 995 cm^{-1} (Si-O stretching), 923 cm^{-1} (Si-O-Al bonds), 876 cm^{-1} (vibration of CO_3^{2-}), 659 cm^{-1} (Si-O-Si bending vibration) and band at 519, 459 cm^{-1} (deformation of SiO_4 tetrahedra).

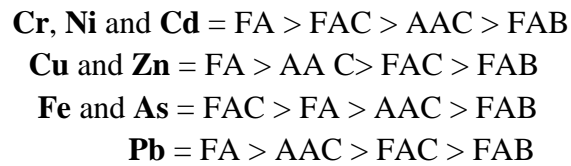
5.9 Heavy metals in fly ash bricks (FAB), blocks (AAC) and cement (FAC)

The collected fly ash bricks (FAB), fly ash blocks (AAC) and fly ash cement (FAC) samples were analyzed for chromium (Cr), iron (Fe), nickel (Ni), copper (Cu), zinc (Zn), arsenic (As), cadmium (Cd). The results for the heavy metal analysis of FAB, AAC and FAC are given in Table 4.40. Results of the selected heavy metals showed that Cr, Fe, Ni, Cu, Zn, As, Cd and Pb are present and their concentration vary widely among these samples (Fig.4.38). The concentrations ($\mu\text{g/g}$) of toxic elements Cr, Fe, Ni, Cu, Zn, As, Cd and Pb found 17.98, 521.34, 11.50, 9.37, 16.68, 3.01, 1.07 and 5.60 in FAB, 47.19, 895.42, 32.42, 34.72, 57.00, 4.64, 1.25 and 19.49 in AAC and 49.46, 948.77, 34.53, 12.37, 34.22, 11.30, 1.28 and 5.55 in FAC samples respectively. Among the trace

elements, it was found that the elements are present in FAB, AAC and FAC samples in order of



A comparison of the results with the values, for FA, FAB, AAC and FAC are given in Table 4.41 and Fig.4.39. This comparison result show that present of elements in FA, FAB, AAC and FAC samples in order of



5.10 Leaching of toxic metals from fly ash (FA), fly ash bricks (FAB), fly ash blocks (AAC) and fly ash cement (FAC)

The experimental results on leaching of toxic metals from FA, FAB, AAC and FAC under varying condition, leaching test were tabulated and plotted to observe trends in the leaching patterns. The toxic metals found on the surface of the fly ash particles are the most readily available candidates for their release into the aqueous environment (Prasad and Mondal, 2008). The release of heavy metals from the surface of fly ash and fly ash materials (FAB, AAC and FAC) depends on the pH of the aqueous medium. The effects of the leaching medium and the important process parameters such as time, pH and solid-liquid ratio on the dissolution of elements from FA, FAB, AAC and FAC have been studied. Leaching of the some selected metals such as Fe, Cr, Cu, Ni, Cd and Pb were observed under sequential batch leaching test and long-term leaching test.

5.10.1 Sequential batch leaching test (SBLT)

The time evolution of the pH of the leachates of different leaching media (acidic, neutral and alkaline) at a different soil-liquid ratio (1:5, 1:10 and 1:20) for fly ash and fly ash materials (bricks, blocks and cements) are given in Table 4.42 through 4.65 and graphically presented in Fig. 4.40 through 4.63. Leaching was done in four cycles

spanning a seven-day period. The change of pH of leachates in successive cycle is mainly governed by the amount as well as mobility of calcium in the samples. Only a small change of pH is observed even when distilled water is used as the leachant indicating low leachability of calcium in the sample.

5.10.1.1 Leaching of toxic metals from FA, FAB, AAC and FAC by SBLT

The leaching process strongly depends on pH of the medium. For each of the metals studied in this study, the influence of pH on leaching is discussed below with respect to the fly ash and fly ash materials (FAB, AAC and FAC). The mobility of different elements in leaching mediums of varying pH at different solid-liquid ratios is given in Table 4.42 through 4.65 and graphically presented in Fig. 4.40 through 4.63. Sequential batch leaching in four cycles covering seven days cycle was done for a solid-liquid ratio of 1:5, 1:10 and 1:20.

Leaching of chromium (Cr)

Chromium in its state of hexavalent oxidation i.e. chromate or dichromate, is widely recognized as potentially carcinogenic and highly soluble in aqueous environment (Huggins and Huffman, 2004), while the trivalent Cr (III) is less soluble and much less problem to human health. It appears that chromium appears in most bituminous coals as Cr^{3+} in organic association and mainly as Cr^{3+} in illite (Goodarzi et al., 2008, Huggins and Huffman, 2004), while there is little evidence of the presence of Cr^{6+} (Huggins et al., 1999). Several authors estimated the fractional state of Cr^{6+} oxidation in fly ash at <5% (Goodarzi et al., 2008, Huggins et al., 1999). Dubikova et al., 2006 reported slightly higher mobility for alkaline ash and increased releases with increasing pH.

In this study, the leaching of chromium in fly ash fluctuates over time with acidic medium, neutral medium and alkaline medium. The leachability of chromium rise significantly with time in the leaching process of all three leachant medium. For a medium of initial pH 4.00, the concentration of Fe in the leachate of FA ash is highest in the first extraction cycle (Table 4.42). The concentration decreases in the third extraction cycle, it increases marginally in the fourth extraction cycle.

The leachability of Cr in FA, FAB, AAC and FAC samples in order of FAC > FA > AAC > FAB

The relationship of leachability of Fe with three leachant medium is found in the order as acidic medium > alkaline medium > neutral medium. The concentration of Cr in the leachate of the FA sample was highest in the first extraction cycle started with acidified water of pH 4.00 (Table 4.42 through 4.65). Thereafter it decreased up to the third extraction cycle. The dissolution of main minerals will affect the leaching characteristics of Cr, especially the element absorbed on the surface of the particle. In addition, Cr can exist in Al and Fe oxides and is possible to concentrate in illite clay. Cr can also be enriched in other minerals by the effect of conversion of organic material in the coal.

Leaching of iron (Fe)

The iron contained in the ashes is mainly present as magnetite mixed in various proportions with hematite, although a small proportion can be assimilated into the vitreous matrix (Kukier et al., 2003). Fe elements are not easily released into the environment due to their spinel structure that is highly stable and resistant to atmospheric agents. The iron becomes soluble at $\text{pH} \leq 1.5$ (Seidel and Zimmels, 1998), but the releases are of little amount in relation to the concentration in the fly ash. Leaching levels drastically decrease to slightly acidic values (pH 3-5) and remain very low during the rest of the pH range. Any iron in solution precipitates as amorphous hydroxide in response to an increase in pH values (Warren and Dudas, 1988). Few proportions of Fe have been damaged by fly ash (Ward et al., 2004).

In this study, the leaching of iron in fly ash fluctuates over time with acidic medium, neutral medium and alkaline medium. The leachability does not reach stability in the leaching process in all three leachant medium. For a medium of initial pH 4.00, the concentration of Fe in the leachate of FA ash is highest in the first extraction cycle (Table 4.42). The concentration decreases in the third extraction cycle, it increases marginally in the fourth extraction cycle. The leaching pattern of Fe is somewhat similar to Cr at the initial pH of 4.00 for all four fly ashes.

The leachability of Fe in FA, FAB, AAC and FAC samples in order of $FAC > FA > AAC > FAB$

Fe is easy to enrich in the surface of the fly ash particles. The relationship of leachability of Fe with three leachant medium is found in the order as acidic medium > alkaline medium > neutral medium. The relationship of leachability of Fe with three solid-liquid ratio is found in the order as $1:5 > 1:10 > 1:20$.

Leaching of nickel (Ni)

Nickel was found mainly in the form of oxide in the coal (Goodarzi et al., 2008) and the minerals containing nickel (spinel and illiths) are common in deposits near ultramafic bodies (Ruppert et al., 1996), while Sulfur minerals contain Ni (Finkelman, 1995). The solubility of Ni is markedly sensitive to pH and covers a few orders of magnitude. Up to 10% Ni was removed when the leaching pH 1 was used (Kim et al., 2003). Mobility decreased sharply to 1% in slightly acidic conditions, such as those of TCLP in alkaline and acid ash and water-based leaching tests in fly ash of acidic nature (Ward et al., 2004).

In this study, the leaching of nickel in fly ash fluctuates over time with acidic medium, neutral medium and alkaline medium. The leachability does not reach stability in the leaching process in all three leachant medium. For a medium of initial pH 4.00, the concentration of Ni in the leachate of FA ash is released faster at the beginning followed by slower dissolution in the last cycle (Table). The concentration decreases in the third extraction cycle, it increases marginally in the fourth extraction cycle. The leaching pattern of Cr at the initial pH of 4.00, 7.00 and 10.00 for all samples are given in Table.

The leachability of Ni in FA, FAB, AAC and FAC samples in order of $FA > FAC > AAC > FAB$

The relationship of leachability of Ni with three leachant medium is found in the order as acidic medium > alkaline medium > neutral medium. The relationship of leachability of Ni with three solid-liquid ratio is found in the order as $1:5 > 1:10 > 1:20$.

Leaching of copper (Cu)

Approximately 2-5% of the total Cu is leached at $\text{pH} \leq 3$ from fly ash samples (Kukier et al., 2003). This observation, suggests that Cu shows a certain degree of mobility in an acidic environment, regardless of the mode of occurrence. Querol et al., 1996 reported a remarkably variable mobility depending on the mode of occurrence in the original coal. A dominant association with clay minerals in coal results in a primary association of glass in fly ash (Spears, 2004). Therefore, copper is assimilated in glass and is not easily released. On the other hand, the oxidation of the Cu-Fe sulphides in the coal leads to a greater mobility of the Cu in the fly ash. The Cu mobile fraction under environmental conditions was estimated at 2.6% (Soco and Kalembkiewicz, 2007). However, Cu was leached to a greater extent in acid extraction, since the releases increased by a few orders of magnitude.

The leaching of copper studied in the FA, FAB, AAC and FAC with acidic medium, neutral medium and alkaline medium increase significantly with time. The concentration of Cu in the leachates of FA is maximum in the first extraction cycle for a medium of initial pH 4.00 (Table) and fourth extraction cycle where less soluble. Its concentrations in the leachates of FAB, AAC and FAC acidic medium of the same initial pH of 4.00 (Table) were found to increase from the first extraction cycle to the fourth. The leachability of Cu fluctuates over time with acidic and alkaline medium. The leachability does not reach stability in the leaching process in acidic and alkaline medium. It is seen that leachability of Cu is higher when the sample is mixed with the acidic medium.

The leachability of Cu in FA, FAB, AAC and FAC samples in order of $\text{FA} > \text{AAC} > \text{FAC} > \text{FAB}$

The relationship of leachability of Cu with three leachant medium is found in the order as acidic medium $>$ alkaline medium $>$ neutral medium. The relationship of leachability of Cu with three solid-liquid ratio is found in the order as $1:5 > 1:10 > 1:20$.

Leaching of cadmium (Cd)

Environmental concerns related to Cd derive from its potential solubility and toxicity in aquatic systems. However, fly ash is depleted in Cd compared to other trace elements (except Hg) and this environmentally sensitive element is constantly immobile in almost neutral and alkaline conditions. Despite its association with the surface of fly ash particles, water leachate concentrations rarely exceed 0.01 mg /kg in alkaline fly ash (Medina et al., 2010, Moreno et al., 2005), while the values of acid fly ash are equivalent to 0.1 mg/ kg at pH ~ 4 (Jankowski et al., 2004, Ward et al., 2009) . Cadmium is somehow leached in acidic conditions, but still scarcely extracted. Solubility decreases towards almost neutral conditions, which result in detectable concentrations under TCLP conditions. The Cd remains practically immobile in a pH range above 7, although some authors have observed a mild amphoteric behaviour.

In this study the leachability of Cd in all three leachants (acidic, neutral and alkaline) is not stable and has no significant difference in leaching in different solid-liquid ratio solution. The leachability does not reach stability in the leaching process in any of the leachant medium. The leachability of Cd is found slightly higher when the sample is mixed with the extraction solution. Some studies indicate that Cd is rich in the surface of fly ash particles so it is easy to leach out. The concentration of Cd leaching for initial pH 4.00 was highest in the first extraction cycle as expected and then decreased very rapidly and reached a low concentration in the fourth extraction cycle. The leaching pattern of Cd in in FA, FAB, AAC and FAC samples in order of FA > FAC > AAC > FAB

The relationship of leachability of Cd with three leachant medium is found in the order as acidic medium > alkaline medium > neutral medium. The relationship of leachability of Cd with three solid-liquid ratio is found in the order as 1:5 > 1:10 > 1:20.

Leaching of lead (Pb)

It is estimated that around 50-60% of Pb is associated with the fly ash surface (Spears and Martinez-Tarrazona, 2004), although the results of Warren and Doubts, 1988 suggest that Pb is most likely to be associated with the glassy interior of the matrix of fly ash and therefore, not easily leachable even in prolonged acidic climatic conditions. Pb is highly

insoluble and virtually immobile (<1% and often <0.1%) in fly ash samples, both acidic and alkaline, regardless of pH and leaching test (Kim et al., 2003, Moreno et al., 2005, Praharaj et al., 2002, Ward et al., 2004). It is believed that the solubility of Pb decreases to a minimum around pH 9, and therefore shows a marked increase at pH > 11.5 after the formation of soluble anionic hydroxy complexes (Jones, 1995).

In this study, the leachability of Pb fluctuates over time for the entire leaching medium. The leachability does not reach stability in the leaching process in any of the leachant medium. The leachability of Pb is slightly higher when the fly ash is mixed with the extraction solution. Lead has the tendency to enrich in the surface of the fly ash particles. The concentration of Pb in the leachate of the sample was the highest in the first extraction cycle, started with acidified water of pH 4.00 (Table). It decreased in other cycles thereafter. For a medium of initial at different pH 4, 7 and 10 the concentration of Pb in the leachates increases from the first extraction cycle to the second and then decreases up to the fourth cycle (Table). The leaching pattern of Pb in FA, FAB, AAC and FAC samples in order of FA > FAC > AAC > FAB

The relationship of leachability of Pb with three leachant medium is found in the order as acidic medium > alkaline medium > neutral medium. The relationship of leachability of Cd with three solid-liquid ratio is found in the order as acidic 1:5 > 1:10 > 1:20.

5.10.2 Long-term leaching test (LTLT)

Long term leaching test (LTLT) performed on the FA, FAB, AAC and FAC. The representative samples of the materials were analyzed under three environmental conditions (acidic, neutral and alkaline) at a different solid-liquid ratio (1:5, 1:10 and 1:20). Each set of sample were extracted with different leaching medium for six month. The leachate samples were collected at different period of time (15d, 30d, 60d, 90d, 120d, 150d and 180d). Seven samples were prepared for each leaching medium and solid-liquid ratio for six month and extracted separately for the determined period.

5.10.2.1 pH of the leachate

The effects of different leaching mediums, solid–liquid ratio and contact time on the leaching of elements from the FA, FAB, AAC and FAC samples were studied under long-term static leaching conditions. Long-term leaching behavior is extremely important for the assessment of environmental risk or impact associated with use of fly ash for land fill or for back-filling of mines or in construction materials (Kumar V., Sharma, 1998).

The changes of pH with contact time in the leachate fly ashes are reported in Table. Data were collected at an interval of 20 days. It is found that for a particular solid–liquid ratio of 1:5, 1:10 and 1:20 pH of the leachate increase with time up to about 120 days thereafter remains almost constant up to 180 days for an initial pH 4 of the leachant. A similar pattern of pH change is noticed for other solid–liquid ratio as well as for an initial pH of 7.0 and 10 of the medium. But, in case of neutral medium leaching, up to 15 days the pH of the leachate changed from 6.6 to 7.7 and thereafter remained virtually constant even up to 180 days. So, on the basis of these data, one may expect that the equilibrium will reach after 120 days in case of acid leaching of some of the elements and 15 days for distilled water leaching.

5.10.2.2 Effect of leaching medium

The effect of different leaching mediums (acidic, neutral and alkaline) at static leaching conditions for a solid–liquid ratio (1:5, 1:10 and 1:20) was studied for each of the fly ash fly ash materials samples to measure the mobility of elements. The concentrations of metals increase with time up to 180 days indication that equilibrium in dissolution reactions is not reached even in such a long contact time. The relationship of leachability of metals with three leachant medium is found in the order as acidic medium > alkaline medium > neutral medium.

5.10.2.3 Leaching of toxic metals

The concentration of metals in the leachate of sample increase with increasing contact time up to 60 days and thereafter decreases over the rest of the contact period of 180 days. In long term leaching test the leachability of Cr and Fe in FA, FAB, AAC and FAC

samples in order of $FAC > FA > AAC > FAB$, the leachability of Ni, Cd and Pb in FA, FAB, AAC and FAC samples in order of $FA > FAC > AAC > FAB$ and the leachability of Cu in FA, FAB, AAC and FAC samples in order of $FA > AAC > FAC > FAB$

5.10.2.4 Effect of solid–liquid ratio

The effect of solid–liquid ratio in the range of 1:5, 1:10 and 1::20 was studied on the long-term static leaching of FA, AAC, FAB and FAC at initial pH Of 4.00, 7.00 and 10.00. The results presented in Table. The relationship of leachability of metals with three solid-liquid ratio is found in the order as $1:5 > 1:10 > 1:20$.